PROCESSING OF MEMPHIS MILLIMETER WAVE MULTI-BASELINE INSAR DATA

Christophe Magnard[1], Erich Meier[1], David Small[1], Helmut Essen[2] and Thorsten Brehm[2]

[1] Remote Sensing Laboratories, University of Zurich, Switzerland
[2] Fraunhofer FHR, Wachtberg, Germany

1. INTRODUCTION

Cross-track SAR interferometry is a well known technique used to extract the information on topography out of SAR images. The selection of the baseline for conventional interferometric systems is a tradeoff: a wide baseline delivers high sensitivity to vertical heights, but there will be many height ambiguities on the interferogram, leading to a difficult phase unwrapping process; with a narrow baseline, the height sensitivity is lower, but there will be fewer ambiguities on the interferogram. Multi-baseline SAR interferometry combines the advantages of narrow and wide baselines.

2. MEMPHIS SAR SYSTEM

MEMPHIS [1] (Multi-frequency Experimental Monopulse High-resolution Interferometric SAR) is a millimeter wave high resolution SAR system, developed and operated by the German research institute Fraunhofer FHR. It operates simultaneously at the 35 GHz- and 94 GHz radar bands, with a bandwidth of 800 MHz, using a synthetic stepped-frequency chirp. This provides a slant range resolution better than 0.2 m. MEMPHIS is typically mounted on a C-160 Transall airplane, flying at relatively low altitude (300 m to 1000 m above ground level). The collected data typically have a 600 m swath width, and can be up to 3 km long in the azimuth direction.

Both 35 GHz and 94 GHz interferometric multiple baseline antennas work with one transmitting horn and four receiving horns. The horns are displaced with respect to each other vertically, allowing single pass multi-baseline cross-track interferometry. The longest baselines are 0.275 m for the 35 GHz antenna and 0.16 m for the 94 GHz antenna.

3. PROCESSING METHOD

We process and focus the SAR raw data to obtain single look complex (SLC) images. The same parameters are used to focus the SAR data from each horn. We use range-Doppler, Ω-k or extended chirp scaling algorithms to produce the SLC images. We tested two multi-baseline processing algorithms.

The first method is described in [2] and [3], whereby the shorter baselines are used exclusively to assist the unwrapping of the longest baseline interferogram. A comparison of different multi-baseline methods is made in [4]. In this comparison, the best results are obtained with the ML (maximum likelihood) processor. It consists of directly using the array of SLC data and finding the optimum phase using a ML estimator [5]. The resulting interferogram may still contain height ambiguities, related to the smallest baseline between the phase centers. This can be easily unwrapped with a conventional phase unwrapping algorithm. We use the statistical-cost network-flow algorithm for phase unwrapping SNAPHU [6].

We use the aircraft navigation data and tie points to transform the range and azimuth position and their phase difference value into a digital surface model (DSM). The differential phase is described by (1), with δ_i the projection of the baseline vector $\overrightarrow{B_i}$ on the look vector $\overrightarrow{r_{1,i}}$ (2) (see [7]). The parameter p depends on the interferometric mode (p = 1 for common transmitter mode, p = 2 for ping pong mode). The data are processed in a zero-Doppler geometry. We choose an orthonormal basis with one of the basis vectors being the normalized linearized velocity (the others are cross-track and normal basis vectors). Expressing $\overrightarrow{r_{1,i}}$ and $\overrightarrow{B_i}$ in this coordinate system (3) enables simplifying approximations.

$$\phi_i = \frac{2p\pi}{\lambda} \cdot \delta_i - \phi_{const} \qquad (1)$$

$$\delta_i = \left\|\overrightarrow{r_{2,i}}\right\| - \left\|\overrightarrow{r_{1,i}}\right\| \cong -\frac{\overrightarrow{r_{1,i}} \cdot \overrightarrow{B_i}}{\left\|\overrightarrow{r_{1,i}}\right\|} \qquad (2)$$

$$\overrightarrow{r_{1,i}} = \begin{pmatrix} r_{1v,i} \\ r_{1c,i} \\ r_{1n,i} \end{pmatrix}, \ \overrightarrow{B_i} = \begin{pmatrix} B_{v,i} \\ B_{c,i} \\ B_{n,i} \end{pmatrix} \qquad (3)$$

$$\left\|\overrightarrow{r_{1,i}}\right\| = \sqrt{r_{1v,i}^2 + r_{1c,i}^2 + r_{1n.i}^2} \cong \sqrt{r_{1c,i}^2 + r_{1n.i}^2} \qquad (4)$$

$$\delta_i \cong -\frac{\overrightarrow{r_{1,i}} \cdot \overrightarrow{B}}{\left\|\overrightarrow{r_{1,i}}\right\|} = -\frac{1}{\left\|\overrightarrow{r_{1,i}}\right\|} \cdot \begin{pmatrix} r_{1v,i} \\ r_{1c,i} \\ r_{1n,i} \end{pmatrix} \cdot \begin{pmatrix} B_{v,i} \\ B_{c,i} \\ B_{n,i} \end{pmatrix} = -\frac{\left(r_{1v,i}B_{v,i} + r_{1c,i}B_{c,i} + r_{1n,i}B_{n,i}\right)}{\left\|\overrightarrow{r_{1,i}}\right\|} \cong -\frac{\left(r_{1c,i}B_{c,i} + r_{1n,i}B_{n,i}\right)}{\left\|\overrightarrow{r_{1,i}}\right\|} \qquad (5)$$

With the help of at least one tie point, combining equations (1), (4) and (5), we can determine ϕ_{const} and then compute the geographical position and height for each point. A regridding is subsequently required to rasterize the DSM.

5. EXPERIMENTAL RESULTS

InSAR flight campaign experiments with MEMPHIS have been carried out in 2009 in a mountainous area in the Swiss Alps and in an urban area near Zurich. Fig. 1 presents results obtained over a highway roundabout near Zurich. Quantitative results comparing the InSAR DSM with a LIDAR digital ground model will be included in the final version of the paper. A masking of features like forests or buildings will be done to ensure directly comparable results. Results from other data takes will also be presented.

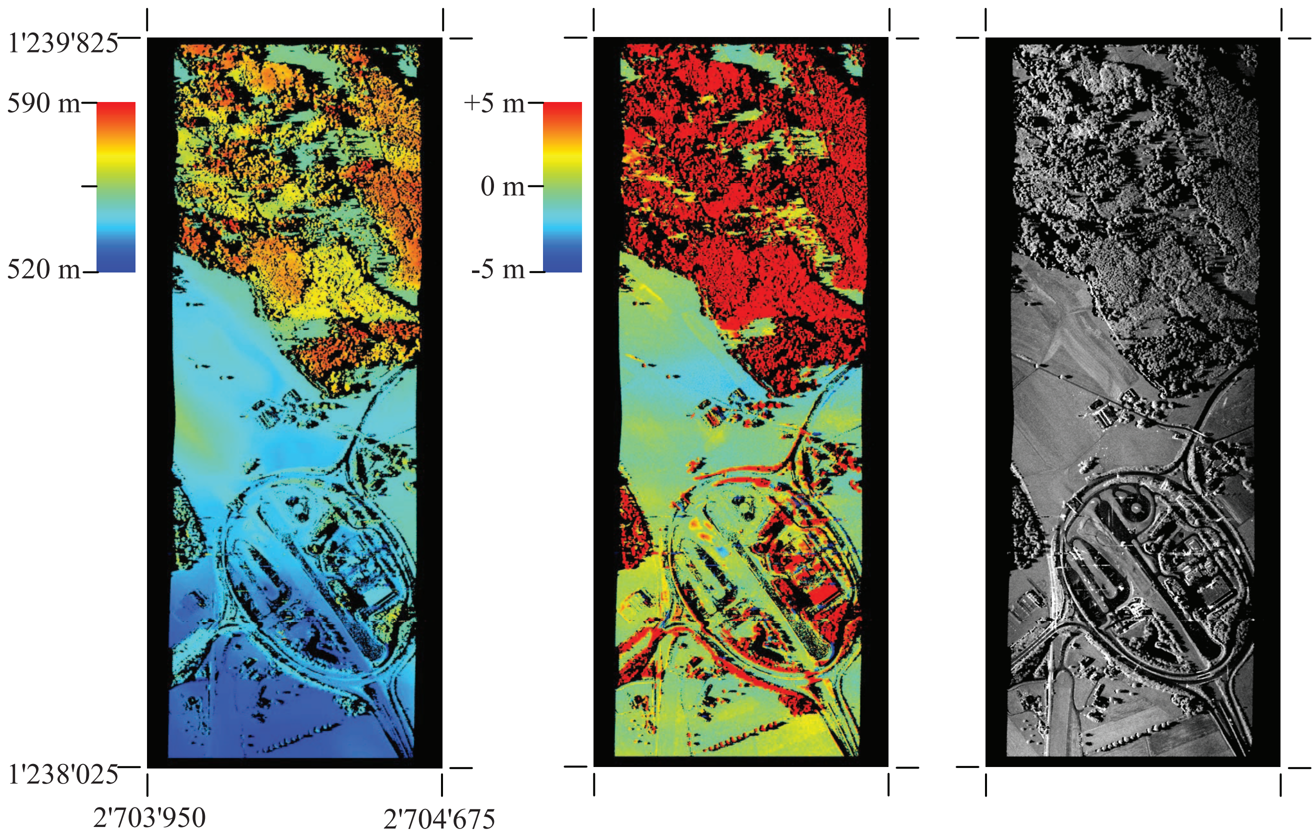

Fig. 1 Results obtained with the 35 GHz over a highway roundabout at Hinwil, Switzerland. Data are shown in the swiss cartographic reference system LV95: (a) the generated DSM, (b) comparison between the InSAR DSM and a reference LIDAR digital ground model, (c) terrain geocoded SAR image produced using the generated DSM.

6. DISCUSSION

The main difficulty with airborne InSAR is producing precise and accurate products with imperfect navigation data. A further difficulty with MEMPHIS is that it is a removable system, with the antenna pod inclined depending on the data take characteristics. Highly precise measurements (compared to the wavelength) of the lever arms/baseline vector are therefore not possible. Our approach to overcome these difficulties is to process the data from the four receivers using the same lever arm. The receivers are displaced in the direction perpendicular to the look vector; remaining errors in the look direction are far smaller than the range sample interval and therefore do not affect the SAR data coregistration. Aircraft attitude data are used to compute the local baseline at each pixel position during the phase to DSM conversion. ϕ_{const} also corrects indistinguishable constant errors in the baseline vector. The smallest azimuth undulations are generated with the above method. In the near future, the methods described in [8] and [9] will be tested as well.

Usage of the ML algorithm for the multi-baseline processing turned out to be more difficult than expected. With such small baselines, particularly the smallest available ones, requirements on the absolute accuracy of their distance measurement are very high. This is less problematic while effectively using only the longest baseline (the smaller baselines being only used for the phase unwrapping), as in our initial method. The results presented to date were therefore obtained with the first method.

7. REFERENCES

[1] H. Schimpf, H. Essen, S. Boehmsdorff, T. Brehm, "MEMPHIS – A Fully Polarimetric Experimental Radar", Proceedings of the IEEE International Geoscience and Remote Sensing Symposium IGARSS, vol. 3, pp. 1714-1716, June 2002.

[2] H. Essen, T. Brehm, S. Boehmsdorff, U. Stilla, "Multibaseline Interferometric SAR at Millimeterwaves, Test of an Algorithm on Real Data and a Synthetic Scene", Proceedings of SPIE, vol. 6746, Sept 2007.

[3] C. Magnard, E. Meier, M. Rüegg, T. Brehm, H. Essen, "High Resolution Millimeter Wave SAR Interferometry", Proceedings of the IEEE International Geoscience and Remote Sensing Symposium IGARSS, July 2007.

[4] F. Lombardini, H.D. Griffiths, "Optimum and Suboptimum Estimator Performance for Multibaseline InSAR", EUSAR 2000 Special Issue, Frequenz, Zeitschrift für Telekommunikation (Journal of Telecommunications), 55:114-118, March/April 2001.

[5] P. Lombardo, F. Lombardini, "Multi-baseline SAR Interferometry for Terrain Slope Adaptivity", IEEE Proc. Nat. Radar Conf. 1997, pp. 196-201, New York, May 1997.

[6] C.W. Chen, "Statistical-Cost Network-Flow Approaches to Two-Dimensional Phase Unwrapping for Radar Interferometry", PhD Dissertation, Department of Electrical Engineering, Stanford University, 2001.

[7] P.Rosen, S.Hensley, I. Joughin, F. Li, S. Madsen, E. Rodriguez, R. Goldstein, "Synthetic Apertur Radar Interferometry", Proceedings of the IEEE, vol. 88, no. 3, pp. 333-381, March 2000.

[8] P. Prats, J.J. Mallorqui, "Estimation of azimuth phase undulations with multisquint processing in airborne interferometric SAR images", IEEE Transactions on Geoscience and Remote Sensing, vol. 41, no. 6, pp. 1530-1533, 2003.

[9] P. Prats, A. Reigber, J.J. Mallorqui, "Interpolation-Free Coregistration and Phase-Correction of Airborne SAR Interferograms", IEEE Geoscience and Remote Sensing Letters, vol. 1, no. 3, pp. 188 - 191, 07/2004.